Folded-diagram nucleon-nucleon potential for application to the many-body problem

J. Haidenbauer and Karl Holinde

Institut für Kernphysik, Kernforschungsanlage Jülich, D-5170 Jülich, Germany

Mikkel B. Johnson

Los Alamos National Laboratory, Los Alamos, New Mexico 87545

We calculate an energy-independent nucleon-nucleon potential using the folded-diagram expansion following closely the philosophy for selecting one- and two-meson-exchange terms that led to the successful Bonn energy-dependent interaction. Coupling parameters are very similar in the two cases, as is the reproduction of the scattering phase shifts and deuteron properties, including the electromagnetic form factors. We also present a simpler one-meson-exchange folded-diagram potential. We study the properties of the many-body system using the two energy-independent interactions. The triton is underbound by about 1 MeV, and nuclear matter underbinds at a saturation density considerably above the empirical density, suggesting the need for intrinsic three-body forces. These are considerably different from the properties attributed to the energy-dependent Bonn interactions, reflecting our earlier observation that numerous higher-order corrections need to be considered in the energy-dependent scheme to obtain comparable many-body results.

I. INTRODUCTION

The Bonn potentials determine the nucleon-nucleon interaction in terms of meson exchange. There exist a variety of Bonn one-boson-exchange potentials (OBEP), so called because they are built up from single exchanges of mesons. The most complete ("full") Bonn potential [1] contains, in addition to one-boson-exchange terms corresponding to the known mesons of mass less than 1 GeV, two-meson-exchange pieces that provide the main source of the intermediate-range attraction in the interaction. These potentials generally provide an excellent reproduction of the two-body data.

The full Bonn potential is derived from meson theory using Bloch-Horowitz [2,3] many-body perturbation theory and, as a result, it is energy dependent in addition to having a nonlocal character. Solving the two-body relativistic Schrödinger equation using this potential is a tractable problem, and the solutions have been thoroughly studied. However, in many-body ($n > 2$) systems the situation becomes much more complicated. The difficulties arise from the energy dependence of the interaction. As the potential must be evaluated many times in solving such problems, the calculation can become unacceptably long, especially when two-meson-exchange terms are included.

For the reasons stated above, we will seek to simplify the Bonn potential. We will do this using folded diagrams [4], the method being based on an expansion leading to an energy-independent (or instantaneous, but nonlocal) interaction. Because of its lack of energy dependence, the folded-diagram potential will be advantageous to use in the many-body problem. The method has the additional desirable features that the bookkeeping is expressed diagrammatically and that the diagrams have a close connection, both physically and technically, to those appearing in the Bonn potential. This means that we can make maximal use of the insight gained with the full Bonn potential in constructing our instantaneous potential. Furthermore, the two-body equation of motion is the same in the two cases, which would not be the case with some other well-known methods. Even more importantly, as we showed in a recent paper [5], the convergence of the folded-diagram expansion appears to be enhanced over that of energy-dependent schemes: there exist fewer diagrams to evaluate, and pairwise cancellations reduce the sizes of some of these. For example, the "extrinsic" three-body forces (those which depend on the details of the definition of the potential) are very small because of such a cancellation, which does not occur in the energy-dependent scheme. Analogous cancellations among folded-diagram contributions to effective exchange-current operators arise [4], and these appear to make the expansion of observables simple as well.

Folded diagrams have been developed as a tool for the nucleon-nucleon interaction in a series of papers beginning with a general development [4], followed by a numerical study of the convergence of the folded-diagram expansion for the nucleon-nucleon interaction [6] and a detailed comparison of the structure of the many-body theory with energy-dependent and energy-independent interactions [5]. The retardation that occurs through the energy-dependence in the Bonn potential is reinstated in the instantaneous potential by folded diagrams. In principle, one might expect to pay a price for eliminating the energy dependence, namely, that expansion would not converge to give the correct observables near thresholds. However, rapid convergence to the correct observables has been shown to occur in practice at energies below meson-production threshold in cases where the exact

answer is known [6]. If desired, extension of folded diagrams to the case of inelastic processes can be carried out by going to coupled channels.

In Sec. II we explain the model, discuss the folded-diagram classification, and indicate how we have made our calculations of the folded diagrams. In Sec. III, we present the results, giving the parameters of our energy-independent version of the full Bonn potential together with a simplified OBEP. We also give results obtained with these potentials, for NN scattering below pion-production threshold and for the deuteron state, comparing them to experimental data. In Sec. IV we present results for nuclear matter and the triton with the new interactions. Finally, in Sec. V we summarize our results and draw conclusions.

II. MESON-THEORETICAL TWO-BODY MODEL

In this section, we discuss the physical content of our nucleon-nucleon potential and show how the folded diagrams are evaluated for the potentials used in the calculations that we present in Sec. III. The physical content can be expressed in terms of an underlying field-theoretical Lagrangian. For the Bonn potentials (and extensions to other hadronic systems [7–9]), the Lagrangian is constructed from a selection of mesons and baryons, which interact through specific choices of the meson-baryon and meson-meson couplings. Scattering amplitudes and other observables are expanded perturbatively, and the extended hadron structure is taken into account by including form factors at the meson-meson and meson-baryon interaction vertices.

Our expansion of the potential is guided by the observation that the longest-range components of the interaction correspond to the exchanges of the lightest mesons. This means that the one-boson-exchange (OBE) part of the interaction is built from single exchange of mesons of mass less than 1 GeV, namely, π, η, ρ, ω, σ', and δ. The δ' meson is a representation of $\pi\pi$ interactions (in the 0^+ channel) and is therefore different from $\sigma_{\rm OBE}$ (used in OBE potentials), which effectively parametrizes also uncorrelated $(\pi,\pi)+(\pi,\rho)$ contributions; see Ref. [1]. The two-meson-exchange terms are built from double exchanges of the following pairs of mesons: (π,π), (π,ρ), (π,σ'), and (π,ω). For (π,π) and (π,ρ), we include nucleon as well as Δ intermediate states. As in Ref. [1], we omit (π,η) and (π,δ) because they are quite small, and also $(\rho,\rho),(\sigma',\sigma')$, etc., because they are of much shorter range and because other higher-order terms of the same range are also omitted. Our treatment for (π,σ) exchange is slightly different from that in the full Bonn potential, where the more strongly coupled $\sigma_{\rm OBE}$ was used in (π,σ) exchange. Since we want to avoid problems when going to the equivalent (elastic) $N\overline{N}$ interaction ($\sigma_{\rm OBE}$, according to the above definition, does not have well-defined G parity), we do not follow that procedure here, but use σ' throughout. Antinucleons are omitted, which seems to be a good approximation, at least for pions with pseudovector coupling to nucleons [10].

For the purpose of enumerating the folded diagrams, we use the general classification scheme of Ref. [11]. The

lines that occur in diagrams fall into two categories: active lines (the nucleons), which span the model space, and passive lines (mesons and the Δ), which correspond to excitations outside the model space. Folded diagrams then provide a systematic method for evaluating an Hermitian effective interaction and the corresponding effective operators that act in the model space. Because the interaction is Hermitian and instantaneous, the eigenfunctions of the effective Hamiltonian may be chosen orthonormal, which is one technical advantage over the energy-dependent schemes. The eigenvalues of the effective Hamiltonian give the physical bound-state energies, and the phase shifts give the physical S matrix. Other observables are calculated with the aid of the folded-diagram expansion of effective operators [4,11].

The basic elements of the potential, called "boxes" in the notation of Ref. [11], are connected sets of passive lines. The simplest box is a single meson connecting two nucleons. This fulfills the definition of a box because it is trivially connected. Figure 1 gives the folded diagram corresponding to this box [4]. The complete expression for the folded diagram is found by multiplying its corresponding energy denominator by the appropriate numerator, consisting of meson-nucleon couplings at the vertices. The numerators turn out to be the same as those in Ref. [1], even for the vector mesons [4], if we follow the simplifications of Appendix B of Ref. [1]. The energy denominator, however, is completely different. In the center-of-mass system, it is, for the exchange of meson i,

$$\frac{1}{-\mathbf{q}^2 - m_i^2},\qquad(2.1)$$

where $\mathbf{q}$ is the three-momentum of the meson and m_i is its mass. The potential acts at the time base placed halfway between the times of emission and absorption of the meson as indicated by the horizontal dashed line.

At the two-meson-exchange level there are two types of diagrams that we need to consider. These are the two-meson single-box diagrams and the two-meson double-box diagrams. An example of the former is the "delta box" diagram shown in Fig. 2. This is a single-box folded diagram because the mesons and the Δ form a completely connected set of lines. We also include, following Ref. [1], the two-meson-exchange diagrams containing two Δ's, shown in Fig. 3. All time orderings should be included when evaluating these (and the other) two-meson-
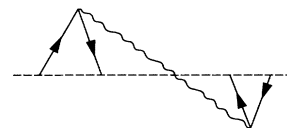
FIG. 1. Folded diagram corresponding to the one-meson-exchange potential. The horizontal line is the time base, which denotes the time at which the instantaneous potential acts relative to the time of emission and absorption of the exchanged meson.

(a)   (b)
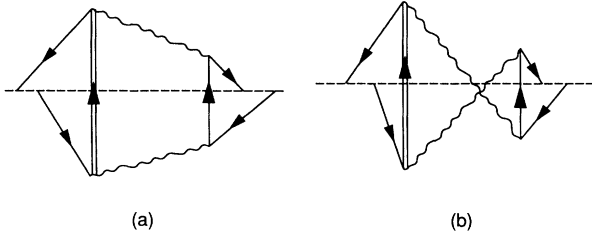
FIG. 2. Single-box folded diagrams containing one Δ: (a) Δ box diagram; (b) a Δ crossed-box diagram. These contribute to the full folded-diagram potential.

exchange folded diagrams.

Figures 2(a) and 2(b) [and Figs. 3(a) and 3(b)] are called "delta box" and "delta crossed-box" diagrams, respectively, in Ref. [1]. These may be evaluated by a straightforward application of the rules found in Ref. [4], in which case each diagram of Fig. 2 is found to consist of a product of energy denominators expressed in terms of four off-shell energy variables conjugate to the times at which the vertices act. Placing the time base at the average of the four times of the vertices corresponds to replacing these off-shell energies by specific combinations of the on-mass-shell energies E_q and $E_{q'}(E_q^2 = q^2 + m_N^2)$ of the nucleons appearing in the initial and final states, respectively, of the potential matrix element. The resulting expression can be rearranged in a convenient fashion to facilitate comparison to the Bonn potential. After this rearrangement, these energy denominators can be identified with the time-ordered diagrams found in Eqs. (B.17) and (B.18) of Ref. [1] for the Δ box and Eq. (B.20) for the Δ crossed-box diagrams. The single-box Δ folded diagrams are equivalent to these terms if we fix the off-shell variable z at

$$z = E_q + E_{q'} . \qquad (2.2)$$

The diagrams have the same numerators as in Ref. [1]. The difference between evaluating the two-meson single-box diagram either as a folded diagram or as a term in the full Bonn potential then becomes just a choice of z. For example, the instantaneous potentials corresponding to D_1^{it} [Eq. (B.17) of Ref. [1] is

$$D_1^{it} = (z - E_{q'} - E_k - \omega_{q'-k})(z - E_k - E_k^*)$$

$$\times (z - E_q - E_k - \omega_{q-k}) , \qquad (2.3)$$
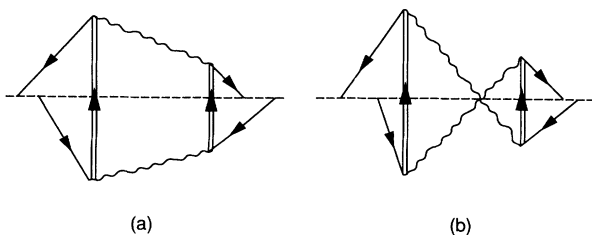
with $E_k^{*2} = k^2 + m_\Delta^2$ and with z given by Eq. (2.2).

The remaining two-meson folded diagrams are double-box diagrams. There are two types, true-correcting and model-correcting folded diagrams. These are both illustrated in Fig. 4. They are not single-box diagrams because they are not completely connected by lines lying outside the model space. Figure 4(a) is true correcting, meaning that it is not generated by an iteration of a single-box folded diagram. The model-correcting diagram, Fig. 4(b), is a piece of the iteration of the single-box folded diagram that is not a valid time ordering of the corresponding Feynman diagram. As such, it must be evaluated and subtracted as a separate term in the potential. As explained above, our model consists of double-box folded diagrams for the following pairs of exchanged mesons: (π,π), (π,ρ), (π,σ'), and (π,ω).

The denominator structure of the true-correcting folded diagram of Fig. 4(a) is identical to the Δ crossed-box diagram in Fig. 2(b) [or Fig. 3(b)], the only difference being the masses of the intermediate particles. These bear the same relationship to the Bonn potential as did the two-meson-exchange single-box diagrams and can be calculated as discussed in connection with Eq. (2.3). Its numerator is identical to the crossed-box diagrams of Ref. [1] for the same set of mesons. The model-correcting folded diagram, Fig. 4(b), is discussed in detail in Refs. [4] and [6]. The short horizontal lines cutting the individual meson lines in the figure are the time base of the one-meson exchange in Fig. 1; the relative time ordering of these lines must be maintained in evaluating this diagram, as must the sense of the internal folded nucleon line (running backward in time). An expression for this folded diagram is found in Refs. [4,5]. As also discussed there, the stretched-box diagrams as defined in Ref. [1] are automatically included in the iteration of Fig. 1 when the time base is chosen as it is in our work.

It is clearly seen from Eqs. (2.2) and (2.3) that the diagrams of Figs. 1–3 and 4(a) on shell ($z = 2E_q = 2E_{q'}$) have values identical to the corresponding diagrams of the Bonn potential [the folded diagram, Fig. 4(b), has no counterpart], and the integration over intermediate momenta in the two-meson diagrams encounters no singularities. However, when they are used as potentials in the two-body scattering equation, they must be evaluated half off shell, and at these points the corresponding terms in the folded diagram and Bonn potentials are no longer

(a)   (b)

FIG. 3. Single-box folded diagrams containing two Δ's: (a) a Δ box diagram; (b) a Δ crossed-box diagram. These contribute to the full folded-diagram potential.

(a)   (b)
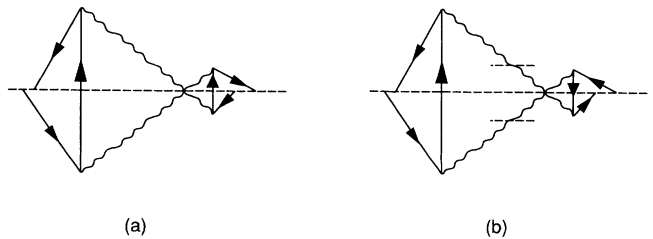
FIG. 4. Double-box two-meson-exchange folded diagrams: (a) a true-correcting double-box folded diagram; (b) a model-correcting double-box folded diagram.

equal to each other. For certain off-shell points, the energy denominators in the folded-diagram potential develop zeros. The occurrence of these zeros is connected with the existence of meson-production thresholds, and the proper way to handle the singularities was specified in Ref. [4], namely, the poles must be integrated as a principal value. When this is done, the overall potential remains finite. The remaining "pole" piece of the diagrams corresponds to meson production and is therefore justifiably neglected in the energy region below meson-production threshold.

The principal value causes no problem in principle, but in practice it makes the diagrams lengthy to evaluate. Results evaluated in this fashion were obtained in a stable calculation and presented in Refs. [4,5]. In the present work we found that the calculation of some of the diagrams became more difficult to stabilize, due to the merging of two singularities in the (three-dimensional) integration over the intermediate momenta in Figs. 2–4. For this reason, we have looked for approximation schemes that allow us to evaluate these folded diagrams quickly and accurately on the computer.

One can see technically the origin of these zeros by looking at a typical energy denominator in a higher-order diagram [see Eq. (2.3)],

$$\frac{1}{z - E_{q'} - E_k - \omega_{q'-k}} . \qquad (2.4)$$

When z is replaced as in Eq. (2.2), this denominator becomes

$$\frac{1}{E_q - E_k - \omega_{q'-k}} . \qquad (2.5)$$

The problem arises in Eq. (2.5) when q becomes very large compared to q'. In this case, the denominator can vanish for some value of the loop momentum k. This can be avoided if E_q is replaced by $E_{q'}$. It can be shown that denominators occur in pairs with E_q and $E_{q'}$ appearing symmetrically, so that after this approximation the potential retains the Hermitian character of the unapproximated folded diagram. In general, there remain slight changes in the off-shell matrix elements of the potential; however, their effect on NN observables turns out to be almost negligible for the cases that have been compared to the exact principal-value integration. This is not surprising, since off-shell contributions occur only in higher-order interactions, which we know to be quite small.

We have found that one additional problem occurs in connection with the Δ box diagrams. If we follow the prescription outlined above, the size of the folded diagram becomes radically larger off shell than that of the corresponding term of the Bonn potential. We have traced this difference to a rather strong energy dependence of the box diagram near Δ production threshold, which arises from the term $z - E_k - E_k^*$ in the box propagators of Eq. (B.17) of Ref. [1] [cf. also Eq. (2.3)]. The additional energy dependence generated by the other two terms in the propagator is quite weak throughout the whole energy range. We therefore divide the box into

two contributions, a main contribution (defined by setting $z = 2m_N$ in the term $z - E_k - E_k^*$) and a remaining piece. The latter piece, however, is quite small below threshold for Δ production and can therefore safely be neglected. We then replace the smooth energy dependence, stemming from the other two terms in the propagator, by an instantaneous potential according to the folded-diagram procedure. Indeed, we find that below meson-production threshold, this procedure reproduces the results of the full Bonn potential to within a few percent. We would be able to do a complete folded-diagram calculation, including the neglected piece, by enlarging the model space to include Δ's. This would lead naturally to coupled channels, which we consider in a future publication.

III. RESULTS FOR THE NUCLEON-NUCLEON SYSTEM

A. Parameters

In this section, we construct two potentials: a "full" folded-diagram potential including two-meson-exchange contributions, FULLF, and a one-boson-exchange version of it, OBEPF. The full folded-diagram potential was obtained by fitting the meson-nucleon coupling parameters appearing in the expressions of Sec. II to the two-body observables. To obtain OBEPF, the two-meson-exchange terms of the full potential were replaced by a fictitious scalar meson σ_{OBE}, and small compensating adjustments were made in some of the parameters of the other one-meson-exchange terms. We would naturally expect that the meson-theoretical couplings found for the full potential would be closer to their true values, but we establish in Sec. IV that OBEPF is nevertheless useful as an expedient for exploring the implications of the full interaction in the many-body problem.

The resulting meson parameters for our full folded-diagram potential are given in Table I, together with corresponding values of the full Bonn potential [1]. As we would expect from correctly executed perturbation theory, the parameters of the folded-diagram potential differ only slightly from those of the full Bonn potential. (The only exception is the $N\Delta\pi$ cutoff mass. Since, for stability reasons, we now use a dipole form factor for both $N\Delta\pi$ and $N\Delta\rho$ vertices, we have to increase the $N\Delta\pi$ cutoff mass to 2 GeV in order to obtain the same realistic isobar contributions as in the original Bonn potential.) This fact is reassuring, leading us to conclude that both interactions are acceptable representations of the same underlying meson-nucleon field theory.

Although the lack of energy dependence is an advantage of the full folded-diagram potential, its two-meson-exchange terms are still lengthy to calculate, so we have developed a simplified one-meson-exchange version of it, OBEPF. The construction of OBEPF is similar to that for OBEPT in Ref. [1], except that OBEPT is energy dependent like the full Bonn potential. In both interactions the complicated two-meson-exchange terms of the full Bonn potential are eliminated in favor of a much simpler but fictitious scalar-meson-exchange term. It is not possible to retain the same meson-nucleon coupling parameters, because the two-meson-exchange terms also

TABLE I. Meson parameters applied in our full folded-diagram interaction FULLF. Numbers in parentheses denote corresponding values of the full Bonn potential, when different. Nucleon mass $m = 0.938\,926$ GeV; mass of Δ isobar $= 1.232$ GeV.

Vertex	$I(J^P)$ of meson	Meson mass m_α (GeV)	$g_\alpha^2/4\pi[f_\alpha/g_\alpha]$	Cutoff mass Δ_α (GeV)	η_α
$NN\pi$	$1(0^-)$	0.138 03	14.4	1.2 (1.3)	1
$NN\rho$	$1(1^-)$	0.769	0.74 [6.6] (0.84) ([6.1])	1.25 (1.4)	1
$NN\omega$	$0(1^-)$	0.782 6	25.0 (20.0)	1.6 (1.5)	1
$NN\delta$	$1(0^+)$	0.983	1.9984 (2.8173)	2.0	1
$NN\sigma'$	$0(0^+)$	0.560 (0.550)	6.7761 (5.6893)	1.8 (1.7)	1
$N\Delta\pi$	$1(0^-)$	0.138 03	0.224	2.0 (1.2)	2 (1)
$N\Delta\rho$	$1(1^-)$	0.769	20.643 (20.45)	1.5 (1.4)	2

contribute to the tensor force. Therefore, the tensor force in the one-meson-exchange terms must be strengthened. This was achieved in OBEPT by increasing the cutoff mass in the pion-nucleon form factor from 1300 to 1750 MeV.

The parameters of the OBEPF potential are shown in Table II. Again, these are quite similar to those of OBEPT, shown for comparison in the same table. In particular, the range of the pion-nucleon form factor (1.75 GeV) is the same in the two cases. For both OBE versions, we use a slightly higher mass for σ_{OBE} in $I = 0$ than in $I = 1$. The reason is that the two-meson-exchange contributions, effectively parametrized by σ_{OBE}, are definitely shorter ranged in $I = 0$. (For example, the relatively long-ranged $N\Delta$ box diagrams are absent in $I = 0$.) Note, however, that the $I = 1$ parameters given in Table II also fit the $I = 0$ phase shifts and all deuteron properties. Only the accurate description of the triplet-S low-energy scattering parameters (see below) require the higher σ_{OBE} mass.

TABLE II. Parameters for our folded-diagram interaction OBEPF. The number in square brackets denotes the tensor-to-vector coupling ratio. Where the values for OBEPT differ, they are given in parentheses. For the definition of the parameters, see Ref. [1]. The parameters for σ_{OBE} given in the table apply only to the $I = 1$ NN potential. For $I = 0$ we have $m_\sigma = 0.740$ (0.615) GeV, $g_\sigma^2/4\pi = 18.8742$ (11.7027), and $\Lambda_\sigma = 2.0$ GeV.

Meson	Mass (GeV)	$g_\alpha^2/4\pi$	Δ_α (GeV)
π	0.138 03	14.4 (14.6)	1.75
η	0.548 8	5.0	1.5
σ_{OBE}	0.550	7.9864 (8.8543)	2.0
δ	0.983	3.6276 (1.1585)	2.0
ρ	0.769	0.86 (0.92) [6.1]	1.5
ω	0.782 6	20.0	1.475(1.5)

B. NN scattering phase shifts

The resulting NN scattering phase shifts, derived from the folded-diagram potentials FULLF and OBEPF, are shown in Fig. 5 for $J = 0-2$ and energies below pion-production threshold in comparison to Arndt's phase-shift analysis [12]. This figure also contains the corresponding predictions for the energy-dependent version OBEPT. (The results for the full Bonn potential can be found in Ref. [1].) Obviously, both folded-diagram potentials describe the data fairly accurately; the reproduction is at least of the same quality as in case of the energy-dependent version OBEPT. In some partial waves (e.g., $^1D_2$) there are minor discrepancies at higher energies; however, we will demonstrate in the next section that they do not have any impact on the results for the many-body system derived from these potentials. (Note that application to the many-body system was the primary aim for constructing these folded-diagram potentials.)

C. Deuteron and low-energy parameters

Table III contains the deuteron and low-energy scattering parameters predicted by both folded-diagram potentials. The excellent reproduction of these empirical data [13–17] is essential in view of the later application to the many-body problem. Thus, both versions can be considered as reliable starting points for meaningful nuclear-structure calculations.

There is one striking difference between the present energy-independent and the former energy-dependent versions: FULLF as well as OBEPF have a considerably larger D-state probability compared to both the full Bonn (4.25%) and OBEPT (4.27%) potentials. Since P_D is not an observable this difference is not in contradiction to any data. A larger value was, in fact, anticipated in the energy-independent scheme by Desplanques [18].

At this point it is instructive to compare OBEPF and
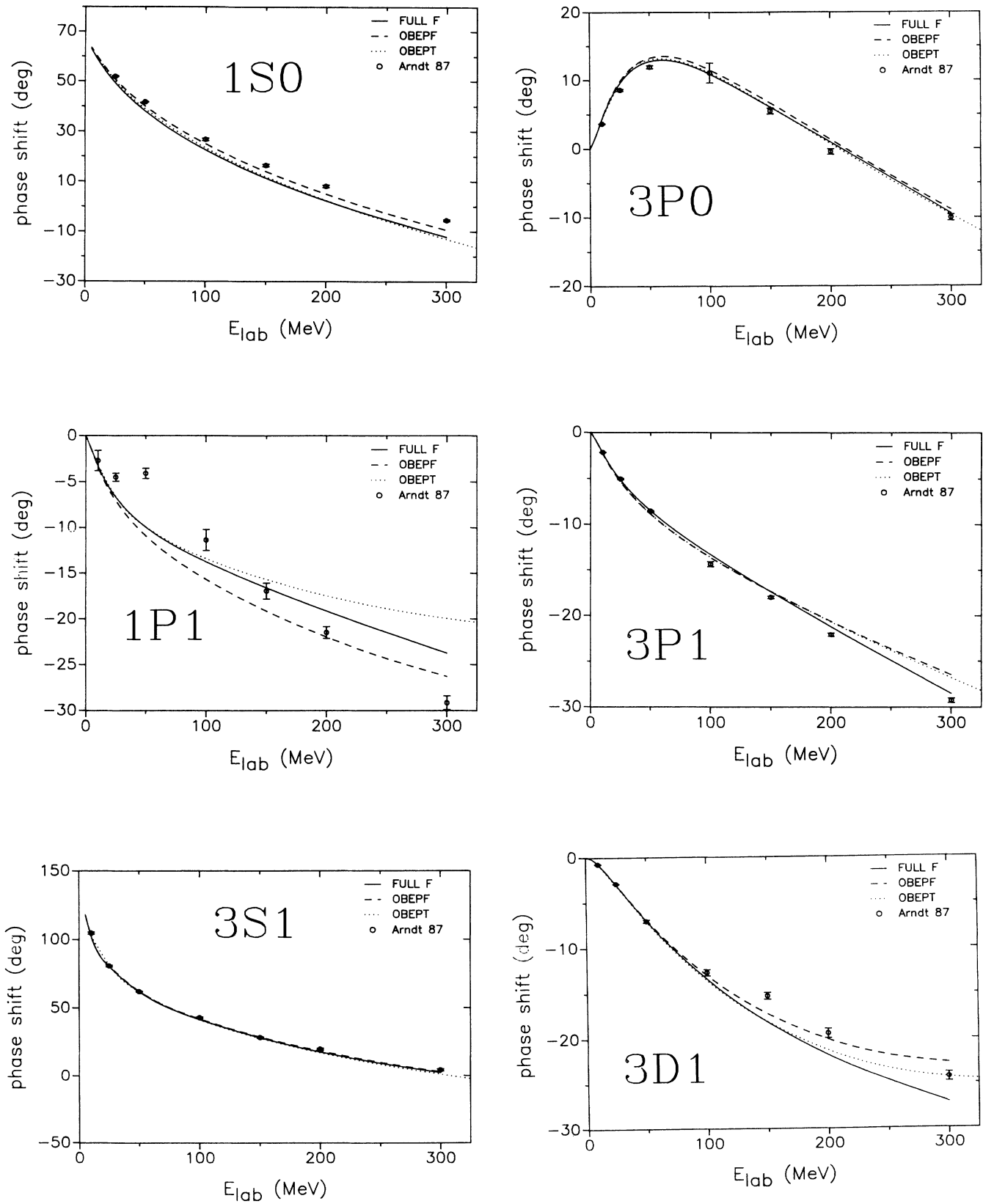
FIG. 5. Selected phase shifts for n-p scattering. The solid curve is the full folded-diagram potential FULLF; the dashed curve corresponds to the one-boson-exchange version OBEPF. The dotted line is the model OBEPT from Ref. [1]. Experimental phase shifts are from Arndt et al. [12].

OBEPQ [1] because these are both instantaneous OBE potentials obtained from somewhat different points of view. The latter was obtained using the Blackenbecler-Sugar prescription [19] truncated at the one-meson level. It was intended to have the same low deuteron D-state probability as the (energy-dependent) OBEPT. This could only be achieved by weakening the tensor force of the one-pion-exchange potential, which was accomplished by decreasing the value of the cutoff mass of the $NN\pi$ form factor to 1.3 GeV. (Although this value hap-
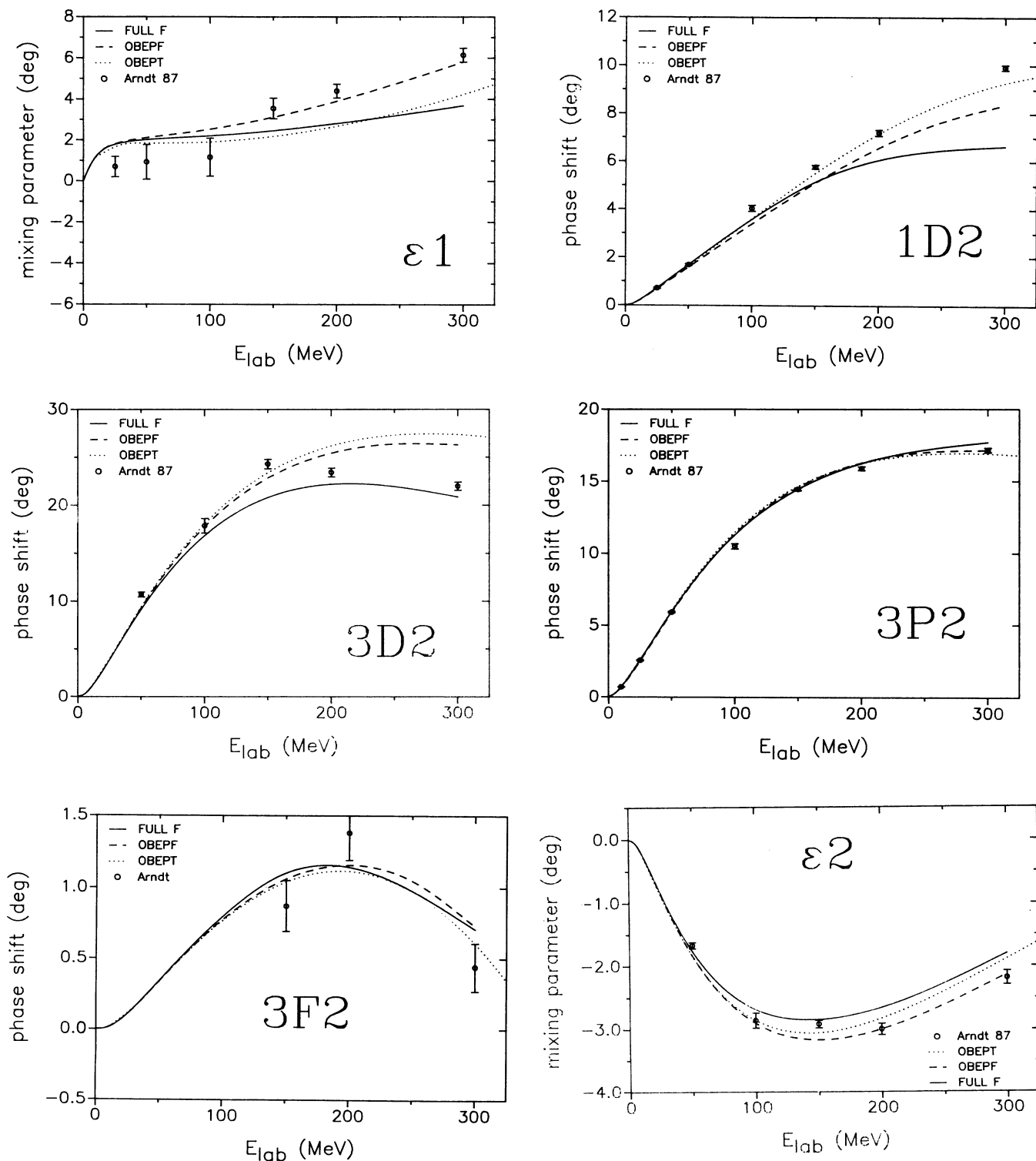
FIG. 5. *(Continued).*

TABLE III. Deuteron and low-energy scattering parameters, predicted by our full folded-diagram potential (FULLF) and by a corresponding one-boson-exchange version (OBEPF), compared with experiment. The experimental values are taken from the references indicated in the footnotes; the low-energy scattering data are from Dumbrajs *et al.* [17].

	FULLF	OBEPF	Exp.
Deuteron			
Binding energy ε_d (MeV)	2.2244	2.2246	2.224 575[a]
D-state probability P_d (%)	5.22	5.66	
Quadrupole moment Q_d (fm^2)	0.2796	0.2805	0.2859±0.0003[b]
Asymptotic S state A_S (fm$^{-1/2}$)	0.8886	0.8867	0.8846±0.0016[c]
Asymptotic D/S	0.0264	0.265	0.0256±0.0004[d]
Neutron-proton low-energy (scattering length a, effective range r)			
$^1S_0$: a_s (fm)	−23.76	−23.75	−23.758±0.010
r_s (fm)	2.812	2.710	2.75±0.05
$^3S_1$: a_t (fm)	5.436	5.426	5.424±0.004
r_t (fm)	1.766	1.754	1.759±0.005

[a]Reference [13].
[b]Reference [14].
[c]Reference [15].
[d]Reference [16].

pens to be the same as in the full Bonn potential, the tensor force in OBEPQ is likewise weaker since the two-meson-exchange terms in the full model increase the tensor force, as discussed before.) Indeed, a comparison of the parameters of OBEPQ (see Table 5 of Ref. [1]) to those of OBEPF, given in Table II, shows that the most significant difference is the smaller $NN\pi$ cutoff mass in OBEPQ, which is responsible for the rather low values for the mixing parameter ϵ_1 at higher energies. We shall see in the next section that this discrepancy in the tensor force between OBEPF and OBEPQ leads to sizable differences in the many-body system.

D. Deuteron form factors

In traditional phenomenological approaches to electron-deuteron (e-d) scattering, the dynamics is described in terms of static, instantaneous NN interaction models. The deuteron form factors are first calculated in the nonrelativistic impulse approximation (IA), and then various corrections, such as relativistic effects (RC) and meson-exchange currents (MEC) computed from effective operators, are added. A similar procedure can be followed in conjunction with our folded-diagram potentials.

Use of the same meson-exchange current for all instantaneous potentials would seem to be inconsistent at first sight, since according to the folded-diagram approach, potential-dependent terms should appear in the exchange-current operators. However, this procedure is approximately justified by virtue of the strong cancellations that occur among the potential-dependent terms at the level of one-meson exchange. Moreover, Friar [20] has calculated explicitly the leading-order (in v/c) non-vanishing exchange-current corrections in various schemes, including folded diagrams, and displayed their equivalence after eliminating the canceling terms. One has thus tended to use the same exchange-current opera-

tor for all instantaneous potentials, regardless of their origin. Accordingly, also for our folded-diagram potential one can take the potential-independent terms from Refs. [21], but we point out that if one wants to take advantage of the systematic folded-diagram classification for calculating corrections at the level of two-meson exchange, one will want to recalculate the potential-independent one-meson-exchange terms following the standard folded-diagram prescription at some future time.

The situation is, however, different for OBEPT and the full Bonn potential from Ref. [1]. The approximate equivalence among exchange-current operators does not hold for energy-dependent potentials, so one cannot use the exchange-current calculations of Ref. [21] for the aforementioned models. Furthermore, the wave function nonorthonormality resulting from such energy-dependent interactions provide even a serious conceptual problem in connection with these traditional approaches. Therefore it is clearly advantageous to use our folded-diagram potential also for investigations in the e-d system.

In the following we demonstrate the effect of the energy dependence (or, equivalently, the wave function nonorthogonality) by means of an IA calculation. Figure 6 shows the deuteron form factors $A(q)$ and $B(q)$ (see, e.g., Ref. [22] for their definitions) obtained with the folded-diagram potential FULLF in comparison to the full model of [1] and experiments [23–29]. In this calculation we employed the empirical dipole fit given by Gari and Hyuga [21(b)] for the nucleon form factor. The curves for the full Bonn model correspond to the deuteron wave function given in Ref.[1], where orthonormality was imposed by simply renormalizing the NN part to unity (cf. footnote a of Table 3 in Ref. [1]). For both the electric and the magnetic deuteron form factors the predictions of FULLF lie above the ones for the full Bonn potential. This shift has to be attributed to the energy independence of the folded-diagram potential.

We want to mention at this point that there is also a more phenomenological prescription for dealing with energy-dependent potentials in e-d scattering suggested by Friar [30]. According to him the effects of the energy dependence of an interaction model $V(E)$ on the pertinent NN wave function Ψ can be eliminated via the transformation

$$\hat{\Psi} = \left[1 - \frac{\partial V}{\partial E}\right]^{1/2} \Psi , \qquad (3.1)$$

leading to an orthonormalized wave function $\hat{\Psi}$, which then can be used in the standard way. Indeed, this procedure was applied to the full Bonn NN model in Ref. [31]. They found that the elimination of the energy dependence leads to a shift in the predicted form factors, an effect which is in fact comparable to the result we obtained by applying the folded-diagram prescription. Thus, our calculations tend to confirm qualitatively the findings of Pauschenwein et al. [31]. Clearly, the systematic removal of the energy dependence via the folded-diagram expansion is theoretically much more appealing than the ad hoc prescription of Eq. (3.1), since only the former does allow a consistent treatment of

meson-exchange currents (cf. the comments above).

A similar shift in the deuteron form factors was found also in an analogous comparison of OBEPF and OBEPT. Note that the discrepancies between the predictions of FULLF and the data, in particular for higher-momentum transfer, are not an indication for shortcomings of our model. After RC and MEC are added to our IA results shown in Fig. 6 (which can be done unambiguously for the folded-diagram models), the predictions should come up to the experimental values [31].

IV. THREE-BODY SYSTEM AND NUCLEAR MATTER

We have found that only small adjustments in the parameters of the folded-diagram interaction are needed to achieve the same quality fit to empirical data as the Bonn interactions. Since this is the case, we can expect [5] that the properties of many-body systems calculated with the folded-diagram interaction are equivalent to those that would be obtained with the full energy-dependent Bonn potential. (We assume that these small relative adjustments compensate for the higher-order diagrams that have been omitted.) We are therefore able to bypass the more complicated many-body theory that occurs in the
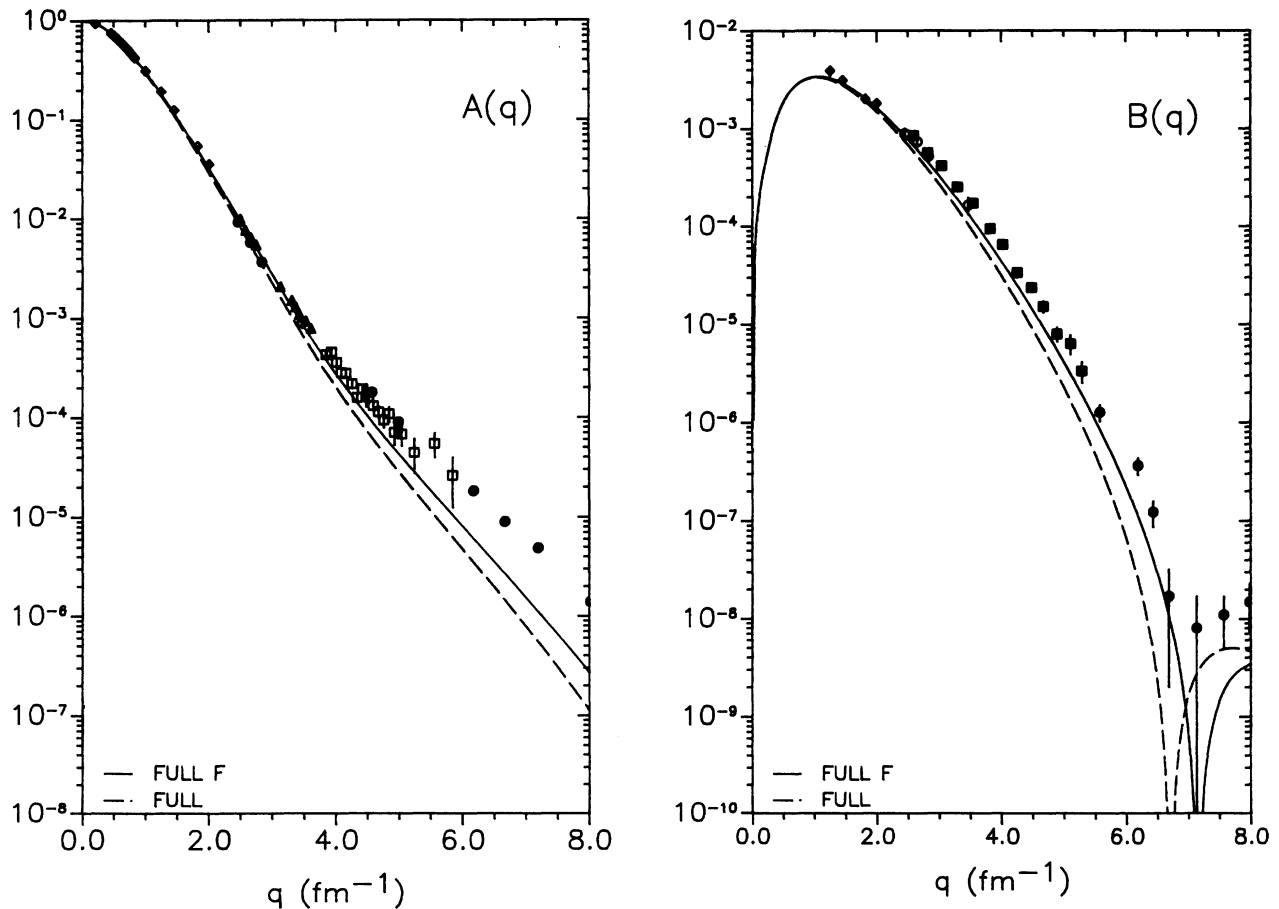
FIG. 6. Deuteron electric and magnetic form factors calculated in impulse approximation. The solid curve is the full folded-diagram potential FULLF; the dashed curve corresponds to the (energy-dependent) full Bonn potential given in Ref. [1]. Experimental data are from Refs. [23–27] [for $A(q)$] and from Refs. [23,27–29] [for $B(q)$].

energy-dependent scheme by using our folded-diagram interaction.

A. Nuclear matter

In lowest order (two-hole-line approximation) the binding energy E of nuclear matter is given by

$$E = \sum_m \langle m|h_0|m \rangle + \tfrac{1}{2} \sum_{m,n} \langle mn|G(z)|mn - nm \rangle . \quad (4.1)$$

Here, the first term denotes the kinetic-energy contribution; the G matrix depends on the starting energy $z = \varepsilon_m + \varepsilon_n$ and is obtained from a solution of the Bethe-Goldstone equation

$$G = V + V\frac{Q}{z-h}G , \quad (4.2)$$

in which Q denotes the Pauli projector and h contains, in addition to the free-particle energy, E_m, single-particle potentials building up the total single-particle energies ε_m. According to the "standard" or "gap" choice, these energies are given by

$$\varepsilon_m = \begin{cases} E_m + \sum_n \langle mn|G(\varepsilon_m+\varepsilon_n)|mn \rangle & \text{for } k_m < k_F , \\ E_m & \text{for } k_m > k_F , \end{cases} \quad (4.3)$$

i.e., the G matrix has to be determined self-consistently.

Figure 7 shows the resulting binding energy per particle, E/A, as a function of the Fermi momentum k_F. Both folded-diagram potentials, in spite of their completely different physical structure, yield quite similar results, which, moreover, agree qualitatively with those obtained from comparable instantaneous interactions. Table IV demonstrates that slight differences between the two model predictions occur in all partial-wave states. Apart from $^3S_1$, these can be completely traced to small differences in the corresponding phase-shift descriptions
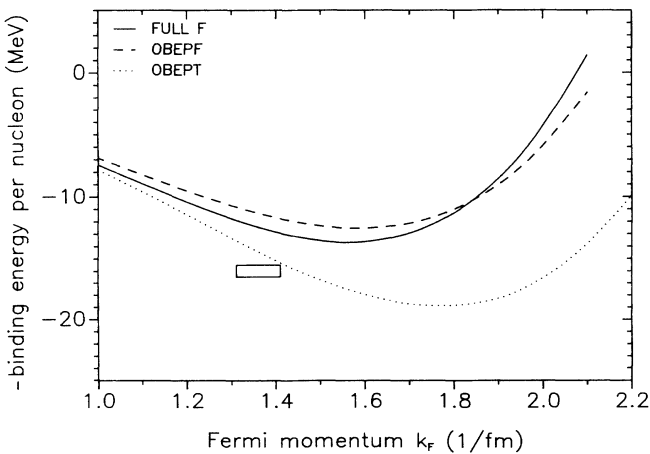
FIG. 7. The total binding energy per nucleon as a function of density as measured by the Fermi momentum. Same description of the curves as in Fig. 5. The small box represents the experimental situation.

TABLE IV. Partial-wave contributions (in MeV) to the binding energy of nuclear matter, E/A, for our full folded-diagram potential FULLF, the one-boson-exchange version OBEPF, and the corresponding energy-dependent potential OBEPT at $k_F = 1.5 \text{ fm}^{-1}$.

	FULLF	OBEPF	OBEPT
$^1S_0$	−19.81	−19.94	−19.28
$^3P_0$	−4.67	−4.84	−4.79
$^1P_1$	5.47	6.15	5.36
$^3P_1$	14.93	14.92	14.87
$^3S_1$	−21.28	−20.48	−23.45
$^3D_1$	2.38	2.19	2.11
$^1D_2$	−3.83	−3.62	−3.79
$^3D_2$	−5.74	−5.83	−6.03
$^3P_2$	−10.35	−10.26	−10.92
$^3F_2$	−0.90	−0.90	−0.91
$J=3$	4.46	4.52	4.42
$J=4$	−2.50	−2.58	−2.64
$5 \leq J \leq 12$	0.76	0.76	0.76
Potential energy	−41.09	−39.91	−44.29
Kinetic energy	27.51	27.51	27.51
E/A	13.58	12.39	16.77

(compare Fig. 5). A detailed inspection of the situation in $^1D_2$ shows that the sizable difference between the phase shifts predicted by FULLF and OBEPF at higher energies ($E_{\text{lab}} > 150$ MeV) does not have any impact on the nuclear-matter results since this difference would suggest a lower binding for FULLF in this partial wave. However, FULLF provides even more binding, which demonstrates clearly that the nuclear-matter results are determined by the behavior of the phase shifts below 100 MeV only. (Indeed, FULLF provides a larger $^1D_2$ phase shift in that region.)

As expected, in the energy-independent scheme, the two-body cluster contributions do not provide sufficient binding and saturate at relatively too high a density. The situation is different in the energy-dependent framework. As Fig. 7 shows, OBEPT provides too much binding on the two-body cluster level. As seen from Table IV, the increased binding arises essentially from the $^3S_1$ state, due to the drastically smaller deuteron D-state probability of OBEPT.

The deviations from the empirical value suggest the need for three-body (and possibly higher-body) clusters and three-body forces. More importantly, to the extent that we are using (essentially) the same meson-nucleon field theory for the energy-dependent and energy-independent potentials, leading in principle to the same result, the discrepancy between the theoretical predictions in both schemes on the two-body cluster level implies that many-body clusters and three-body forces have quite different characteristics in the energy-dependent and energy-independent framework. Thus, potentials defined in different schemes, which lead to different results on the two-body cluster level, should converge to the same result as higher-order contributions are includ-

ed. Conversely, the fact that, in lowest order, an instantaneous potential predicts about the same result as an energy-dependent potential does not mean that the final results will likewise be the same. In fact, this is highly unlikely since the higher-order contributions behave quite differently in both schemes, as demonstrated in Ref. [5] for the extrinsic three-body forces.

Thus, although OBEPQ provides overbinding comparable to OBEPT on the two-body cluster level (the two having a similar deuteron D-state probability), we should expect the final results evaluated from both potentials, including higher-order contributions, to be completely different. In this sense, and in contrast to OBEPF, the energy-independent OBEPQ potential is *not* equivalent to OBEPT or the full Bonn potential in spite of having about the same (low) D-state probability.

We have some understanding of the many-body cluster contributions in the energy-independent scheme. These have been examined by Day [32]. We also understand from Ref. [5] that one class of three-body forces [33], the "extrinsic" ones, is small for instantaneous interactions. The residual intrinsic three-body forces are very interesting, and our most likely source of information about them is a comparison between calculations and measurements of ground-state properties of many-nucleon systems.

Adding the multibody cluster contributions from Day [32] and taking the extrinsic three-body forces to be negligible for the folded-diagram interaction [5], we find that nuclear matter saturates at $k_F \approx 1.6$ fm^{-1} with $E/A \approx -18$ MeV. Since these are not the empirical values of the Fermi momentum and binding energy, we conclude that additional terms, either intrinsic three-body forces or some other dynamics (e.g., relativistic effects), must also contribute. These results are, in a sense, the most important ones of the present paper, since our previous analysis [5] shows that an equivalent calculation within the framework of the energy-dependent scheme is quite difficult and is unlikely to be made in the near future.

B. Three-body system: the triton

The difficulties caused by the energy dependence become especially severe when the full Bonn interaction is used for finite systems. Some of these problems were anticipated [1], which is one reason that the energy-independent potential OBEPQ has been constructed. This potential and variants thereof have been used extensively in the three-body calculations [34,35]. Since our folded-diagram potentials OBEPF and FULLF have a substantially different D-state probability than OBEPQ, we look at their implication for the triton in this section.

Faddeev calculations for the trinucleon bound state were performed for the so-called five-channel configuration (only the $^1S_0$ and $^3S_1$-$^3D_1$ partial waves are used as NN input). Such a five-channel calculation provides already the bulk of the triton binding energy and therefore suffices for the present purposes. Furthermore,

comparable results for essentially all modern NN models are available in the literature [35,36]. Higher partial waves do contribute somewhat differently depending on the particular NN model; however, they do not lead to qualitative modifications (in general, they increase the binding energy by only about 0.1 to 0.3 MeV).

We solve the three-body (Faddeev) equations in momentum space by first performing a separable finite-rank expansion of the NN sector. Such a technique has been previously studied extensively by one of the authors (J.H.) [37,38] for the case of the Paris NN potential [39]. In Ref. [37] it was shown that with a separable expansion of sufficiently high rank, convergence on the three-body level can be achieved. Indeed, in the meantime the three-body results obtained with this separable-expansion method have been confirmed by other groups using different techniques—for the trinucleon binding problem [36] as well as for the continuum [40]. For the models FULLF and OBEPF we followed closely the procedure described in Ref. [37], and we refer the reader to this paper for further details. Again it turned out that separable representations of rank 4 for $^1S_0$ and rank 6 for $^3S_1$-$^3D_1$, respectively, are sufficient to get converged results.

The triton binding energies obtained in our five-channel calculation are 7.86 MeV for FULLF and 7.83 MeV for OBEPF. These values agree, in fact, perfectly with the expectation expressed in our preceding paper (cf. Sec. IV C therein) [5] but are substantially smaller than the corresponding result for OBEPQ (8.36 MeV) [35]. As compared to OBEPF the full folded-diagram potential provides slightly more binding of the triton since its deuteron D-state probability is smaller. In fact, this effect could have been more pronounced; it is, however, for the most part compensated by the somewhat less attractive $^1S_0$ partial wave of FULLF (cf. Fig. 4).

Comparable (five-channel) calculations for other instantaneous NN potentials like, e.g., the Paris and the Argonne V_{14} [41] models yielded 7.30 and 7.44 MeV, respectively [36]. These values deviate to some extent from the triton binding energies predicted by our folded-diagram models which, however, can be easily understood. The Paris NN potential has a slightly larger D-state probability (5.77%) than FULLF and OBEPF, which is partly responsible for the lower binding energy. Most importantly, however, contrary to our models its $^1S_0$ partial wave is fitted to p-p data; it is known that the additional attraction present in the ($^1S_0$) n-p case produces an enhancement of 0.3 to 0.4 MeV in the binding of the triton. The Argonne potential, on the other hand, has a significantly larger D-state probability, namely, 6.08%.

Again, as in the case of nuclear matter, the number of higher-order effects that need to be included with the folded-diagram potential is relatively small, giving us some expectation that the results we obtain here accurately reflect the implications of the underlying meson theory. Note also, that now, in contrast to the situation for OBEPQ, the theoretical trinucleon binding energy is considerably smaller than the experimental value of 8.48 MeV, so that there is enough room for contributions from intrinsic three-body forces.

V. SUMMARY AND CONCLUSIONS

There are several important motivations for constructing nucleon-nucleon potentials. One of these is to determine the parameters characterizing the underlying effective meson-nucleon field theory by comparing solutions of the two-body Schrödinger equation to the empirical data. Another is to facilitate testing the implications of meson theory for n-body systems.

The first of these goals has been accomplished already with the full Bonn interaction. To explore the implications of the full Bonn potential for the many-body system is, however, a very difficult task. One reason for this is the energy dependence and the complicated nature of the two-meson-exchange terms in the interaction, which make many-body calculations computationally very lengthy. Another reason is that there are many terms to be evaluated in the many-body theory.

For these reasons we have constructed alternative potentials using folded diagrams. We have obtained a full folded-diagram interaction, FULLF, and an approximate one-boson-exchange interaction, OBEPF. The folded-diagram method is used because it leads to an energy-independent interaction. For the two-body problem, we have found that the values of the coupling constants and form factors are comparable to those of the corresponding energy-dependent Bonn potentials, confirming that the same underlying meson-nucleon field theory is being applied in the two cases. By virtue of its lack of energy dependence, the computational time involved in many-body calculations is much shorter with the folded-diagram interaction than with the full Bonn potential. The structure of the many-body theory is also simpler in the case of the folded-diagram interaction because there are fewer terms in higher order and the extrinsic three-body forces tend to cancel out of the folded-diagram po-

tential. For these reasons, we believe that we have made realistic estimates of the binding energy of nuclear matter and the triton based on the common meson-nucleon field theory.

The results of our binding energy calculations for nuclear matter and the triton are 12.56 MeV (at $k_F = 1.58$ fm^{-1}) and 7.83 MeV for OBEPF, respectively, and 13.73 MeV (at $k_F = 1.55$ fm^{-1}) and 7.86 MeV for FULLF, respectively. We note, in particular, that these values are different from the results calculated earlier [1,35] with OBEPQ. The difference can be traced to the substantially lower D-state probability of OBEPQ. We have obtained the larger D-state probability of OBEPF and the full folded-diagram interaction when we demand the best fit of the meson-nucleon coupling parameters to the experimental two-body data.

Since our nuclear-matter and triton observables are different from the empirical values, we conclude that the intrinsic three-body forces [33] will be important. One should calculate these with the parameters corresponding to the full folded-diagram potential (or the full Bonn interaction) rather than those of the OBEPF, since some of the parameters of the latter have been renormalized to account for the simpler structure of the potential. Additional information about the couplings in the meson field theory can be obtained from a consistent calculation of exchange currents and other observables in the few-body sector. Such calculations are also possible to do within the framework of the folded-diagram method [4]. We believe that these extensions are interesting directions for future research.

[1] R. Machleidt, K. Holinde, and Ch. Elster, Phys. Rep. **149**, 1 (1987).

[2] C. Bloch and J. Horowitz, Nucl. Phys. **8**, 91 (1958).

[3] D. Schütte, Nucl. Phys. **A221**, 450 (1974).

[4] M. B. Johnson, Ann. Phys. (N.Y.) **97**, 400 (1976).

[5] M. B. Johnson, J. Haidenbauer, and K. Holinde, Phys. Rev. C **42**, 1878 (1990).

[6] K. Holinde, M. B. Johnson, and R. Machleidt, Phys. Rev. C **32**, 1 (1985).

[7] B. Holzenkamp, K. Holinde, and J. Speth, Nucl. Phys. **A500**, 485 (1989).

[8] R. Büttgen, K. Holinde, A. Müller-Groeling, J. Speth, and P. Wyborny, Nucl. Phys. **A506**, 586 (1990); A. Müller-Groeling, K. Holinde, and J. Speth, ibid. **A513**, 557 (1990); D. Lohse, J. W. Durso, K. Holinde, and J. Speth, Phys. Lett. B **234**, 235 (1990).

[9] J. Haidenbauer, T. Hippchen, K. Holinde, and J. Speth, Z. Phys. A **334**, 467 (1989); J. Haidenbauer, T. Hippchen, and K. Holinde, Nucl. Phys. **A508**, 329c (1990).

[10] H. J. Zuilhof and J. A. Tjon, Phys. Rev. C **24**, 736 (1981); Th. Hippchen and K. Holinde, Phys. Rev. C **37**, 239 (1988).

[11] M. B. Johnson and M. Baranger, Ann. Phys. (N.Y.) **62**, 172 (1971).

[12] R. A. Arndt, J. S. Hyslop, and L. D. Roper, Phys. Rev. D **35**, 128 (1987).

[13] C. van der Leun and C. Alderliesten, Nucl. Phys. **A380**, 261 (1982).

[14] D. M. Bishop and L. M. Cheung, Phys. Rev. A **20**, 381 (1979).

[15] T.E.O. Ericson and M. Rosa-Clot, Nucl. Phys. **A405**, 497 (1983); T.E.O. Ericson, ibid. **A416**, 281c (1984).

[16] N. L. Rodning and L. D. Knutsen, Phys. Rev. C **41**, 898 (1990).

[17] O. Dumbrajs et al., Nucl. Phys. **B216**, 277 (1983).

[18] B. Desplanques, Phys. Lett. B **203**, 200 (1988).

[19] R. Blankenbecler and R. Sugar, Phys. Rev. **142**, 1051 (1966).

[20] J. L. Friar, Phys. Rev. C **22**, 796 (1980).

[21] (a) M. Gari and H. Hyuga, Nucl. Phys. **A264**, 409 (1976); (b) **A278**, 372 (1977).

[22] M. I. Haftel, L. Mathelitsch, and H.F.K. Zingl, Phys. Rev. C **22**, 1285 (1980)

[23] C. D. Buchanan and M. R. Yearing, Phys. Rev. Lett. **15**, 303 (1965).

[24] J. E. Elias, J. I. Friedman, G. C. Hartmann, H. W. Kendall, P. N. Kirk, M. R. Sogard, L. P. Speybroeck, and J. K. de Pagter, Phys. Rev. **177**, 2075 (1969).

[25] S. Galster, H. Klein, J. Moritz, K. H. Schmitt, and D. Wegener, Nucl. Phys. **B32**, 221 (1971).

[26] R. G. Arnold, B. T. Chertok, E. B. Dally, A. Grigorian, C. L. Jordan, W. P. Schütz, R. Zdarko, F. Martin, and B. A. Mecking, Phys. Rev. Lett. **35**, 776 (1975).

[27] G. G. Simon, Ch. Schmitt, and V. H. Walther, Nucl. Phys. **A364**, 285 (1981).

[28] S. Auffret *et al.*, Phys. Rev. Lett. **54**, 649 (1985).

[29] R. G. Arnold *et al.*, Phys. Rev. Lett. **58**, 1723 (1987).

[30] J. L. Friar, in *Lecture Notes in Physics* (Springer-Verlag, Berlin, 1979), Vol. 108, p. 455; Phys. Rev. C **12**, 695 (1975).

[31] J. Pauschenwein, L. Mathelitsch, and W. Plessas, Nucl. Phys. **A508**, 253c (1990).

[32] B. D. Day, Phys. Rev. Lett. **47**, 226 (1981); Phys. Rev. C **24**, 1203 (1981); B. D. Day and R. B. Wiringa, *ibid.* **32**, 1057.

[33] See, e.g., B. F. Gibson and B. H. McKellar, Few Body Syst. **6**, 143 (1988).

[34] R. A. Brandenburg, G. S. Chulick, R. Machleidt, A. Pick-lesimer, and R. Thaler, Phys. Rev. C **38**, 1397 (1988).

[35] R. A. Brandenburg, G. S. Chulick, R. Machleidt, A. Pick-lesimer, and R. M. Thaler, Phys. Rev. C **37**, 1245 (1988).

[36] C. R. Chen, G. L. Payne, J. L. Friar, and B. F. Gibson, Phys. Rev. Lett. **55**, 374 (1985); J. L. Friar, B. F. Gibson, and G. L. Payne, Phys. Rev. C **37**, 2869 (1988).

[37] J. Haidenbauer and Y. Koike, Phys. Rev. C **34**, 1187 (1986).

[38] Y. Koike, J. Haidenbauer, and W. Plessas, Phys. Rev. C **35**, 396 (1987).

[39] M. Lacombe, B. Loiseau, J. M. Richard, R. Vinh Mau, J. Côté, P. Pirés, and R. de Tourreil, Phys. Rev. C **21**, 861 (1980).

[40] T. Cornelius, W. Glöckle, J. Haidenbauer, Y. Koike, W. Plessas, and H. Witala, Phys. Rev. C **41**, 2538 (1990).

[41] R. B. Wiringa, R. A. Smith, and T. A. Ainsworth, Phys. Rev. C **29**, 1207 (1984).